104 (2025) 105210

Contents lists available at ScienceDirect

Poultry Science

journal homepage: www.elsevier.com/locate/psj

Synergistic transcriptomic and metabolomic analyses in Zi geese ovaries with different clutch lengths☆

Shengjun Liu [a,1], Jiaxin Yin [a,1], Kexin Cong [a], Shan Yue [b], Yuanliang Zhang [b], Jinyan Sun [b], Xiaofang Ren [a], Ke Jiang [a], Yunuo Liu [a], Xiuhua Zhao [b,*]

[a] College of Animal Science and Veterinary Medicine, Heilongjiang Bayi Agricultural University, Daqing 163319, PR China
[b] Heilongjiang Academy of Agricultural Sciences, Animal Husbandry Research Institute, Harbin 150086, PR China

ARTICLE INFO

Keywords:
Zi goose
Ovary
Transcriptome
Metabolome
Synergistic

ABSTRACT

The clutch is defined as consecutive days of oviposition. Clutch length is an index that reflects ovulation persistence, and is highly correlated with egg production in birds. To identify the genetic markers associated with clutch length in geese, two consecutive experiments were conducted. In the first experiment, 200 Zi geese were selected, all 230 days old, were selected from the same batch and raised individually in the same environment. Data of egg-laying and clutch traits were recorded. After the laying period, three geese with the longest clutch lengths were selected to form the length clutch group (**LCG**) and three geese with the shortest clutch lengths were formed the short clutch group (**SCG**). In the second experiment, the ovaries of six geese were collected for transcriptomic and metabolomic analyses. The results showed that large clutch length (**LCL**) and average clutch length (**ACL**) were positively correlated with egg number (**EN**) ($P < 0.01$; $r = 0.63$ and 0.60, respectively). Large clutch number (**LCN**) was significantly correlated with the peak egg number (**PEN**) ($r = 0.58$, $P < 0.01$) and EN ($r = 0.60$, $P < 0.01$). EN, LCN, LCL, and ACL showed significant differences ($P < 0.01$) between the two clutch length groups. Transcriptomic analysis identified 424 differentially expressed genes (**DEGs**). Functional enrichment analysis revealed that these DEGs were mainly involved in neuroactive ligand-receptor interactions, ovarian steroidogenesis, and calcium signaling pathways. Further, *AVPR1A, FGF14*, and *LHCGR* were predicted as the key genes regulating LCL. Metabolomic analysis identified 349 differential metabolites (**DMs**) in both the positive and negative ion modes. Pyruvate, isocitric acid, D/L-serine, 3-phospho-D-glycerate, succinate, glycine, and glutamic acid were identified as the key metabolites mainly enriched in the signaling pathways of the TCA cycle. Integration of transcriptomic and metabolomic data revealed critical gene-metabolite pairs, including *ACSL4*–phosphoenolpyruvate, implicated in LCL regulation. In summary, this study provides new insights into the genes and molecular markers affecting LCL in Zi geese.

Introduction

Egg-laying potential is associated with the clutch, defined as consecutive days of oviposition. Clutch traits can be used as selection indicators to improve egg production in poultry breeding (Wang et al., 2023). The average clutch length is negatively correlated with the number of clutches; thus, high-producing birds have fewer but longer clutches (Wolc et al. 2010). A large clutch length (**LCL**) refers to the duration of the longest clutch within the largest clutch cycle, the number of eggs laid in this cycle is called the large clutch number (**LCN**) (Bao et al., 2022; Yang et al., 2023a). LCL and LCN are the key indicators of sustainable egg-laying ability in poultry. Moreover, the heritability of LCL is relatively high, making it a primary indicator in breeding selection for goose egg production (Wolc et al., 2019; Wang et al., 2023).

RNA sequencing (**RNA-Seq**) provides complete transcriptional information at the RNA level (Hao et al., 2024). These results have revealed the mechanisms underlying poultry egg production and have been used for the development of molecular markers (Bello et al., 2021;

☆ SECTION: Physiology and Reproduction

* Corresponding author.
E-mail addresses: lsj4396@163.com (S. Liu), 1462615135@qq.com (J. Yin), 3052675106@qq.com (K. Cong), 924634716@qq.com (S. Yue), 497450215@qq.com (Y. Zhang), 1499217641@qq.com (X. Ren), 2995350985@qq.com (K. Jiang), 201817864@qq.com (Y. Liu), yzzxh_007@163.com (X. Zhao).

[1] Shengjun Liu and Jiaxin Yin contributed equally to this work and are considered equal first authors.

https://doi.org/10.1016/j.psj.2025.105210
Received 26 February 2025; Accepted 23 April 2025
Available online 23 April 2025

Yan et al., 2022). Meanwhile, metabolomics is closely related to phenomics and can directly and accurately reflect the physiological state of organisms (Wu et al., 2019; Yang et al., 2021). For instance, a metabolomics study by Yuan et al. (2020) on stearoyl-CoA desaturase during follicular development in geese revealed cholesterol and pantothenic acid or pantothenates as prospective metabolite biomarkers for studying stearoyl-CoA desaturase-related lipid metabolism in goose granulosa cells. Large-scale datasets from transcriptomics and metabolomics analyses in animals have been successfully integrated. Zhan et al. (2022) revealed a complex molecular regulatory network for the quality of Enshi black pigs through a comprehensive analysis of transcriptomics and metabolomics. Xi et al. (2023) discovered potential molecular markers for sternal development in ducks under different feed restrictions through an integrated transcriptome and metabolome analysis.

As the genetic basis of clutch traits in geese is unclear, this study aimed to identify potential molecular markers affecting clutch length by integrating transcriptomic and metabolomic data, to provide theoretical and technical support for the genetic basis of the laying rhythm of geese.

Material and methods

Ethics statement

The study protocol was approved by the Ethics Committee of Science and Technology of Heilongjiang Bayi Agricultural University (Daqing, China) (Number: DWKJXY2024062).

Animals and experimental design

Zi geese (*Anser cygnoides* L., a small breed), approximately 230 days old, with similar physical conditions were used in this study. The experiments were conducted at the Institute of Animal Husbandry, Heilongjiang Academy of Agricultural Sciences, Qiqihar City, Heilongjiang Province, China (latitude: 47°19′; longitude: 123°45′; altitude: 155 m). This study was divided into two consecutive experiments.

Experiment I: 200 Zi geese were kept in a poultry house with windows, raised individually in separate pens under the same environmental conditions, with a stocking density of one goose per square meter under 12 to 15 h of natural light and a temperature of 10 to 28°C. They were fed the same feed; detailed information on the nutritional level of the feed is presented in Table 1. The birds had free access to food and water. After the geese were introduced to the pens in early March 2024, they began to lay eggs successively, reaching their peak egg production by mid-May; the egg-laying rate decreased to 5 % by early July. The egg production of each individual was recorded at 9 a.m. and 16 p.m. each day. The following indicators of body weight (**BW**), age at first egg (**AFE**), egg weight (**EW**), peak egg number (**PEN**), egg number at 53 weeks (**EN**), large clutch number (**LCN**), large clutch length (**LCL**), average clutch number (**ACN**), and average clutch length (**ACL**) were calculated. The definitions and testing methods are listed in Table 2.

Experiment II: The three geese with the longest LCL and the three with the shortest LCL were selected to form the length clutch group (**LCG**) and the short clutch group (**SCG**), respectively. The two groups of geese were transferred to the laboratory. Anesthesia was induced using 1.5 %–3.0 % isoflurane inhalation. Once unconsciousness was confirmed, the carotid artery was swiftly severed to proceed with dissection. Ovarian samples were collected from each goose, placed into sterile cryovials and rapidly frozen in liquid nitrogen. These ovarian samples were used for histological observations, transcriptome analysis, and metabolome analysis.

Table 1
Composition and nutrient levels of basal diets (air-dry basis, %).

Ingredients	Content	Nutrient levels	Content
Corn	61.50	ME/(MJ/kg)[2]	10.92
Soybean meal	25.00	Crude protein	16.02
Rice bran	7.00	Crude fibre	5.60
Wheat bran	3.00	Calcium	0.72
NaCl	0.30	Phosphorus	0.54
Premix[1]	1.00	Lysine	0.80
DL-Met	0.10	Methionine	0.33
$CaHPO_4$	1.10		
Mountain flour	1.00		

[1] The premix contents per kg of concentrate: Zn 60 mg, Cu 50 mg, Mn 80 mg, Fe 50 mg, I 1.6 mg, Se 12 mg, vitamin A 30.000 IU, vitamin E 100 mg, vitamin D_3 100000 IU.

[2] ME is a calculated value, whereas other values are quantified by measurement.

Statistical analyses

The clutch traits of the goose population were analyzed using the Poultry Breeding Information Intelligent Management and Analysis System (developed by Hand Era Technology Co., Ltd., Beijing, China). All experimental data were processed using SPSS software (version 26.0; SPSS Inc., USA). Initially, data were tested for normality and homogeneity of variance. Subsequently, partial correlation analysis was used to examine the interrelations among various parameters, including BW, AFE, EW, PEN, EN, LCN, LCL, ACN, and ACL. Furthermore, an independent samples t-test was conducted to assess the differences in BW, AFE, EW, PEN, EN, LCN, LCL, ACN, and ACL between the LCG and SCG.

Ovary tissue section preparation and histological observation

Goose ovarian tissue was fixed in 4 % paraformaldehyde for 24 h. It was then dehydrated using graded ethanol solutions of varying concentrations and cleared using a clearing agent. Subsequently, the tissues were infiltrated with and embedded in paraffin. Thin sections (3–5 μm) were cut and placed on a biological tissue slide warmer (KD-TI, KIDE, Spain) for baking at 60°C for 30 min. The sections were then dewaxed, rehydrated, stained with hematoxylin and eosin (**H&E**), and sealed with neutral resin. The sections were observed under a microscope (BX53, OLYMPUS, Japan) at 100 × magnification.

RNA extraction and transcriptome analysis

Total RNA was isolated from each LCG and SCG ovary sample using Trizol Reagent (Invitrogen Life Technologies, China); RNA degradation and contamination were detected by electrophoresis on 1 % agarose gels; RNA purity and concentration were determined using the

Table 2
Definitions and abbreviations of the measured traits.

Trait	Abbreviation	Definition
Body Weight	BW	The weight of the goose when it lays its first egg.
Age at First Egg[b]	AFE	The age of a goose when it lays its first egg.
Egg weight	EW	The average weight of three consecutive eggs at the peak of 40 to 45 weeks of laying.
Peak Egg Number	PEN	Egg number of goose aged 35–45 weeks.
Egg Number	EN	Egg number of goose aged 35–52 weeks.
Large Clutch Length[a,b]	LCL	The longest consecutive laying days throughout the laying period.
Large Clutch Number[a,b]	LCN	The number of eggs laid in the large clutch length.
Average clutch number[ab]	ACN	The average number of eggs laid in all clutch laying cycles.
Average clutch length[ab]	ACL	The average of all clutch laying days in the entire laying cycle.

[a] Adapted from Bao et al. (2022).
[b] Adapted from Yang et al. (2023a).

Nanodrop 2000 (Thermo Fisher Scientific, MA, USA); RNA concentration was also checked using the Qubit® 3.0 Fluorometer (Thermo Fisher Scientific, MA, USA); RNA integrity number (**RIN**) and concentration were determined using the RNA Nano 6000 Assay Kit on the Bioanalyzer 2100 system (Agilent Technologies, CA, USA). Total RNA of samples with RIN $\geq$ 7 and 28 S/18 $S \geq 0.7$ were considered as qualified.

A total amount of 3 μg RNA per sample was used as the input material for RNA sample preparation. Sequencing libraries were generated using the NEBNext® Ultra™ RNA Library Prep Kit for Illumina® (#E7530L, NEB, USA) following the manufacturer's recommendations and index codes were added to attribute sequences to each sample. The RNA concentration of the library was measured using the Qubit® RNA Assay Kit on Qubit® 3.0 and the samples were then diluted to 1 ng/μl. The insert size was assessed using the Agilent Bioanalyzer 2100 system (Agilent Technologies, CA, USA), and the qualified insert size was accurately quantified on the StepOnePlus™ Real-Time PCR System (Thermo Fisher Scientific, MA, USA) (Library valid concentration > 10 nM).

To ensure that the number of fragments accurately reflected the gene expression levels, the number of Mapped Reads and the length of the transcripts in the samples were normalized. Fragments per kilobase of transcript per million fragments mapped (**FPKM**) was used as a metric to measure the expression levels of transcripts or genes. Based on the FPKM quantification, we calculated the Pearson correlation coefficient using R programming language (version 4.4.2) to determine the correlation between all pairs of samples.

Nontargeted metabolomics analysis

Chromatography and mass spectrometry data were acquired using a Thermo Fisher Scientific Vanquish ultra-high-performance liquid chromatography system and an Orbitrap Exploris 120 mass spectrometer. ProteoWizard software was used to convert the original data into the mzXML format, and XCMS software was used for peak alignment, retention time correction, and peak area extraction. The data obtained from XCMS underwent structural identification of metabolites, preprocessing, and quality assessment of the experimental data before data analysis. Both locally built and public databases, including the HMDB (Human Metabolome Database) (http://www.hmdb.ca), Metlin (http://metlin.scripps.edu), MassBank (http://www.massbank.jp/), and mzCloud (https://www.mzcloud.org), were used for metabolite identification. By matching the metabolite retention time, molecular mass (fraction mass error < 10 ppm), secondary fragmentation spectrum, collision energy, and other information in the database, the structures of metabolites in the biological samples were identified, and the identification results were strictly checked and confirmed manually. Differentially expressed metabolites were selected using the variable importance in projection (**VIP**) scores from the first two principal components of the orthogonal partial least squares-discriminant analysis (**OPLS-DA**) model, in conjunction with the univariate analysis *p*-values.

Results

Results of laying trait and clutch trait analysis

After removing the outliers using the triple standard deviation rule for each trait, 174 geese with complete laying period records remained. Descriptive statistics for the laying and clutch traits are presented in Table 3. A comparative analysis of egg-laying and clutch traits for different clutch lengths is shown in Table 4. A highly significant difference was observed in the LCL and LCN ($P < 0.01$) between the two groups, with values of 27.33 d and 8.34 d, and 15.0 and 4.67, respectively. The PEN and EN between the two groups was also significantly different ($P < 0.05$).

The correlation analyses of these traits are presented in Table 5. The results showed that LCL and ACL were positively correlated with EN ($P < 0.01$, with $r = 0.63$ and $r = 0.60$, respectively). LCN showed a significantly positive correlation with PEN ($r = 0.58$, $P < 0.01$) and EN ($r = 0.63$, $P < 0.01$).

Table 3
Descriptive statistics for laying and clutch traits.

Trait	N	Mean	SD	Max	Min
BW (kg)	174	3.97	0.46	5.07	3.00
AFE (d)	174	265.76	10.20	297.00	249.00
EW(g)	174	123.65	10.41	156.70	95.03
PEN (n)	174	25.75	7.10	40.00	6.00
EN (n)	174	40.55	10.20	60.00	20.00
LCN (n)	174	17.04	10.14	50.00	1.00
LCL (d)	174	30.24	18.12	94.00	1.00
ACN (n)	174	6.78	6.07	56.00	1.00
ACL (d)	174	11.48	10.62	92.00	1.00

BW: Body weight. AFE: Age at first egg. EW: egg weight. PEN: Peak egg number (35–45 week). EN: Egg number (35–52 week). LCN: Large clutch number. LCL: Large clutch length. ACN: Average clutch number. ACL: Average clutch length.

Table 4
Differences of laying and clutch traits in geese between LCG and SCG.

Item	LCG	SCG
BW (kg)	4.15±0.24[a]	4.16±0.20[a]
AFE (d)	253.67±4.04[a]	256.00±3.61[a]
EW(g)	121.27±1.67[a]	121.82±7.75[a]
PEN (n)	33.67±0.58[a]	17.33±4.62[b]
EN (n)	53.67±0.58[a]	29.67±7.57[b]
LCN (n)	15.00±1.73[a]	4.67±1.53[b]
LCL (d)	27.33±1.53[a]	8.33±3.06[b]
ACN (n)	6.57±1.15[a]	1.90±0.44[b]
ACL (d)	11.63±2.56[a]	2.73±0.91[b]

LCG: Large clutch group. SCG: Short clutch group. BW: Body weight. AFE: Age at first egg. EW: Average egg weight. PEN: Peak egg number (35-45 week). EN: Egg number (35–52 week). LCN: Large clutch number. LCL: Large clutch length. ACN: Average clutch number. ACL: Average clutch length.

[a,b] The means with the same lower-case letters in the column of the same flock do not differ significantly ($P > 0.05$) using the Mann-Whitney test.

Note: This table shows the analysis of differences in the laying traits of six geese between groups.

Histological observation of ovary tissue

Observation of ovarian tissue sections revealed the morphological structures of follicles at various developmental stages and the ovarian stroma. The nuclei appeared blue-purple, whereas the cytoplasm and interstitial components exhibited a light red hue. Within the follicles, oocytes, follicular cells, and the zona pellucida were distinctly observable. The ovaries from the LCG showed good overall development, with normal oocyte maturation and an intact smooth zona pellucida (Fig. 1A–C). In contrast, the SCG exhibited oocytes with a retracted and indented zona pellucida (Fig. 1D–F).

Data analysis of the ovarian transcriptome in Geese with different LCL

To investigate the transcriptional differences underlying LCL variation, RNA-Seq analysis are performed on ovarian tissues from LCG and SCG geese. Box plots of FPKM values for all samples are presented in Fig. 2A, the detailed values of FPKM are shown in Y. The principal component analysis (**PCA**) of the samples is shown in Fig. 2B. PCA revealed distinct clustering between groups, with PC1 explaining 91.8 % of the percentage of variance and PC2 explaining 4.4 %. These findings demonstrate the superior quality of the experimental samples, with minimal intragroup variation and pronounced intergroup differences, indicating a high degree of sample credibility.

Using SCG as the control and LCG as the treatment group, transcriptome analysis revealed 14,148 differentially expressed genes

Table 5
Correlation coefficients of laying and clutch traits in geese.

Item	BW (kg)	AFE (d)	EW(g)	PEN (n)	EN (n)	LCN (n)	LCL (d)	ACN (n)	ACL (d)
BW (kg)	1.00	−0.42**	0.34**	−0.27**	−0.21**	−0.13	−0.12	0.13	0.12
AFE (d)	−0.42**	1.00	−0.21**	−0.62**	−0.41**	−0.21**	−0.20**	−0.08	−0.08
EW(g)	0.34**	−0.21**	1.00	0.22**	0.09	0.18*	0.18*	0.11	0.11
PEN (n)	−0.27**	−0.62**	0.22**	1.00	0.80**	0.58**	0.57**	0.38**	0.39**
EN (n)	−0.21**	−0.41**	0.09	0.80**	1.00	0.60**	0.58**	0.43**	0.43**
LCN (n)	−0.13	−0.21**	0.18*	0.58**	0.60**	1.00	0.99**	0.61**	0.63**
LCL (d)	−0.12	−0.20**	0.18*	0.57**	0.58**	0.99**	1.00	0.60**	0.62**
ACN (n)	0.13	−0.08	0.11	0.38**	0.43**	0.61**	0.60**	1.00	0.99**
ACL (d)	0.12	−0.08	0.11	0.39**	0.43**	0.63**	0.62**	0.99**	1.00

BW: Body weight. AFE: Age at first egg. AEW: Average egg weight. PEN: Peak egg number (35–45 week). EN: Egg number (35–52 week). LCN: Large clutch number. LCL: Large clutch length. ACN: Average clutch number. ACL: Average clutch length. * represents a significant difference; ** represents a very significant difference.
Note: This table shows the correlation analysis results for the laying rhythm of 174 geese.

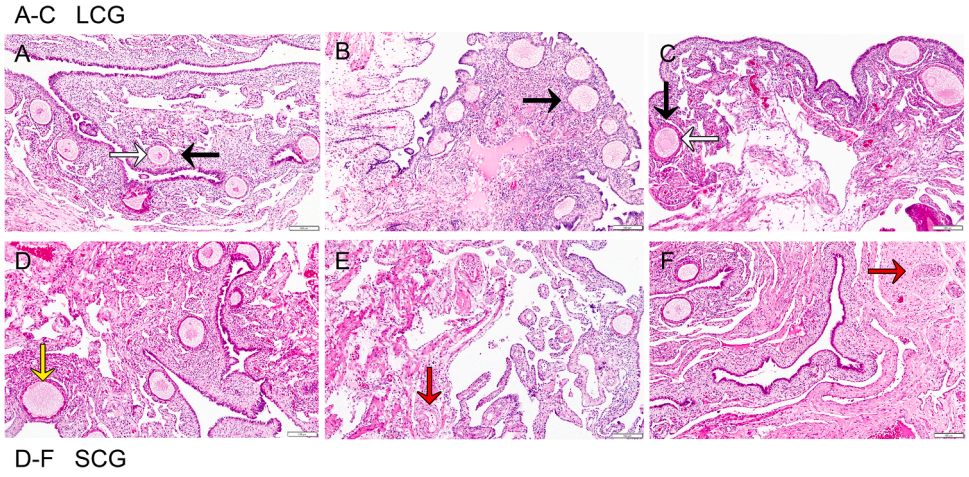

Fig. 1. Observation of ovarian tissue in the length clutch group (LCG) and short clutch group (SCG). (A–C) LCG ovarian tissue sections showing well-developed oocytes (black arrowheads) and intact zona pellucida (white arrows). (D–F) SCG sections with atretic follicles (red arrows) and indented zona pellucida (yellow arrows).
Note: H&E staining;. Magnification, 100×.

(**DEGs**). By applying the thresholds of $|\log_2 \text{Fold Change}| > 1$ and FDR < 0.05, 424 DEGs were screened between the LCG and SCG. Of these, 206 genes were upregulated in the LCG and 218 were downregulated (Fig. 2C). Subsequently, Gene ontology (**GO**) enrichment analysis revealed that DEGs were enriched across 283 GO terms, with notable enrichment in 35 specific terms (Fig. 3A), it includes intrinsic component of membrane, ribonuclease activity, and cell adhesion.

Kyoto Encyclopedia of Genes and Genomes (**KEGG**) enrichment analysis indicated that the DEGs were significantly enriched in 233 pathways. These DEGs were predominantly enriched in neuroactive ligand-receptor interaction, ovarian steroidogenesis, and the calcium signaling pathway (Fig. 3B). The enrichment of key DEGs in GO terms and KEGG pathways is shown in Fig. 3C. By assessing the relative expression levels of DEGs and their relevance to the pathways associated with egg production performance, we identified arginine vasopressin receptor 1A (***AVPR1A***), fibroblast growth factor 14 (***FGF14***), and luteinizing hormone/chorionic gonadotropin receptor (***LHCGR***) as candidate genes that could potentially affect the egg-laying traits of geese. The expression levels of *AVPR1A and FGF14* were upregulated, but *LHCGR* was downregulated in LCG. They are mainly enriched in pathways such as neuroactive ligand-receptor interaction.

Data analysis of the ovarian metabolome in Geese with different LCL

Metabolite extraction and analysis were performed for the LCG and SCG. Box plots of FPKM values for all samples are shown in Fig. 4A. Subsequently, OPLS-DA was applied as a supervised pattern recognition method for multivariate statistical analysis, highlighting pronounced disparities among samples across various groups (Fig. 4B), with R^2Y and Q^2Y approaching 1. suggesting excellent sample congruity and validating the precision and dependability of the model. The PCA score plot revealed divergent metabolic profiles between the LCG and SCG samples (Fig. 4C). These findings demonstrate that the experimental samples utilized for metabolite group analysis were of superior quality and exhibited ample replicability, thus ensuring the trustworthiness of the outcomes for subsequent analyses.

Metabolite profiling was performed using LC-MS techniques, resulting in the identification of 27,224 distinct metabolites across the positive and negative ion modes. Of these, 1,670 metabolites were annotated with their names and classifications using diverse databases. Subsequently, a differential metabolite analysis was conducted to compare LCG and SCG. Applying the criteria of $|\log_2 \text{Fold Change}| > 1$, VIP > 1, and $P < 0.05$, 349 DMs were screened between the LCG and SCG, including 103 upregulated DMs in the LCG and 246 downregulated DMs in the LCG (Fig. 4D). All DMs were tallied and classified, with the top three classifications being organic acids and their derivatives, lipids and lipid-like molecules, and benzenoids. These findings imply that these three groups of metabolites may significant influence the LCL in geese.

KEGG enrichment analysis indicated that these DMs were significantly enriched in 111 metabolic pathways. Five pathways were extremely significantly enriched, including glyoxylate and dicarboxylate metabolism, carbon metabolism, arachidonic acid metabolism, methane metabolism, and TCA cycle (Fig. 5A). The enrichment of DMs

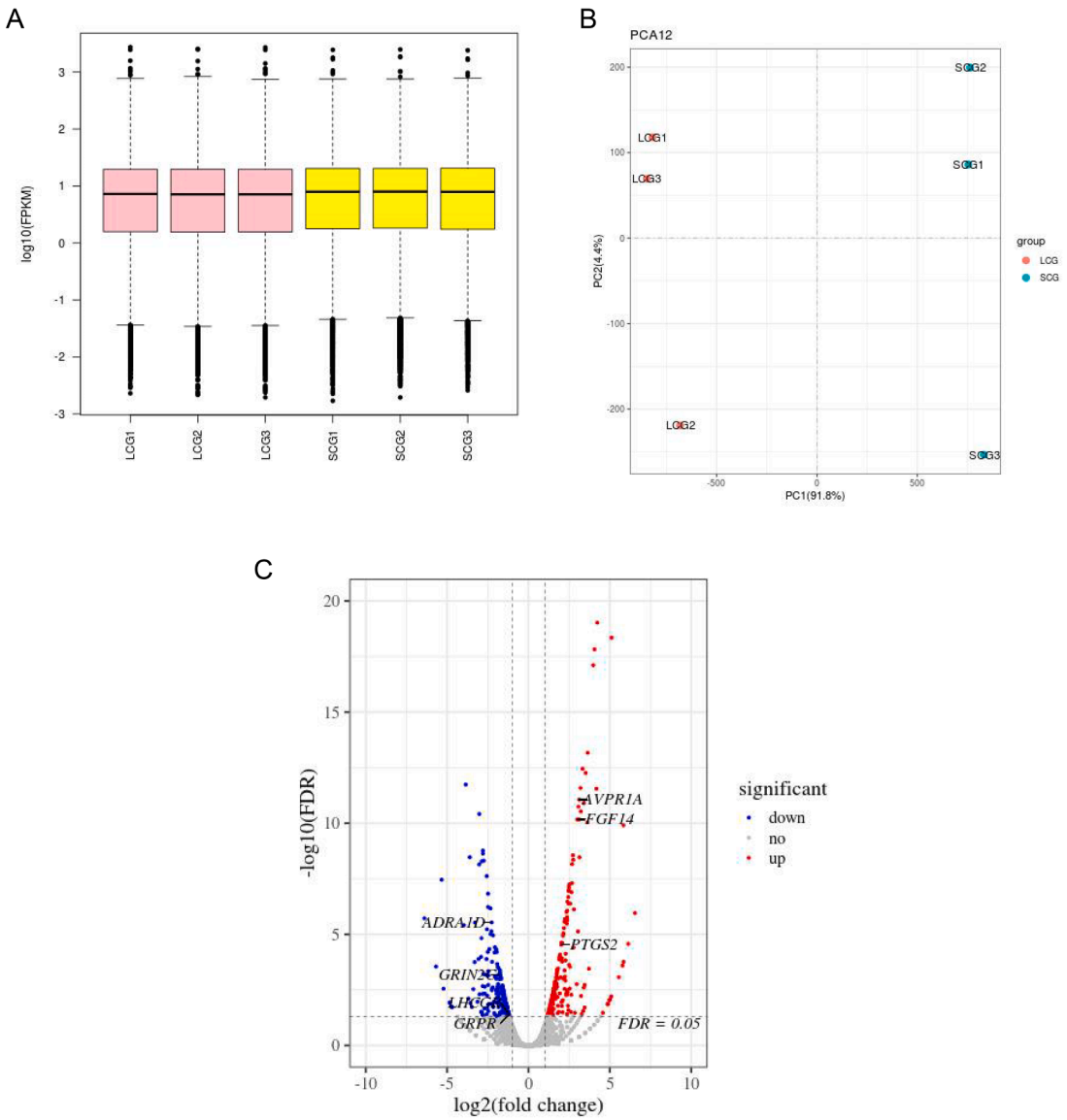

Fig. 2. Quality analysis of transcriptome samples. (A) Fragments per kilobase of transcript per million fragments mapped (FPKM) box plot. The difference in the overall expression of each sample can be measured by density. (B) Principal component analysis (PCA). Each point in the figure represents a sample, with the horizontal coordinate indicating the value of principal component 1 and the vertical coordinate indicating the value of principal component 2. (C) Differentially expressed genes (DEGs) volcano map analysis. The red dots represent upregulated DEGs, and the blue dots represent downregulated DEGs.

in the KEGG pathways is shown in Fig. 5B. Among them, the rich factor of the TCA cycle is 0.6, and several metabolites such as pyruvate, isocitric acid and succinate are enriched in this pathway. According to the DMs of other significantly enriched pathways, we found that pyruvate, isocitric acid, D/L-serine, 3-phospho-d-glycerate, succinate, glycine, and glutamic acid might be the key metabolites affecting egg-laying capacity.

Pathway integration and correlation analysis of DEGs and DMs in the Goose Ovary

To determine the factors influencing LCL in Zi geese, a thorough analysis was conducted by integrating transcriptomic and metabolomic data. DEGs and DMs from the LCG and SCG were subjected to pathway integration and correlation analyses. In the ovarian tissues of both groups, the intersection of enriched pathways derived from DEGs and DMs was illustrated using Venn diagrams and bubble charts for shared pathways (Figs. 6A, B). The findings revealed that DEGs and DMs converged in 24 pathways. Notably, among these 24 pathways, there were no pathways in which both DEGs and DMs were significantly enriched. Pathways such as tyrosine metabolism, amino acid biosynthesis, and arachidonic acid metabolism were the principal routes in which DEGs and DMs were predominantly enriched.

The correlation between DEGs and DMs was analyzed using Pearson calculation. Further, the correlation between all DEGs classified under metabolism in KEGG enrichment and the top 50 DMs was also examined (Fig. 6C). From this figure, we can conclude that the correlation coefficient between Acyl-CoA Synthetase Long-Chain Family Member 4 (***ACSL4***) and phosphoenolpyruvate is relatively high ($r = 0.94$, $P = 0.0048$). Further, the interaction items with correlation greater than $|r| > 0.6$ and $P < 0.05$ (including the correlation between mRNA and mRNA, metabolite and metabolite, and mRNA and metabolite) were extracted and displayed using Cytoscape (version 3.10.0) (Fig. 7).

Discussion

In total, 424 DEGs and 349 DMs were identified. Based on these DEGs and DMs, we predicted *AVPR1A, FGF14*, and *LHCGR* as the key genes

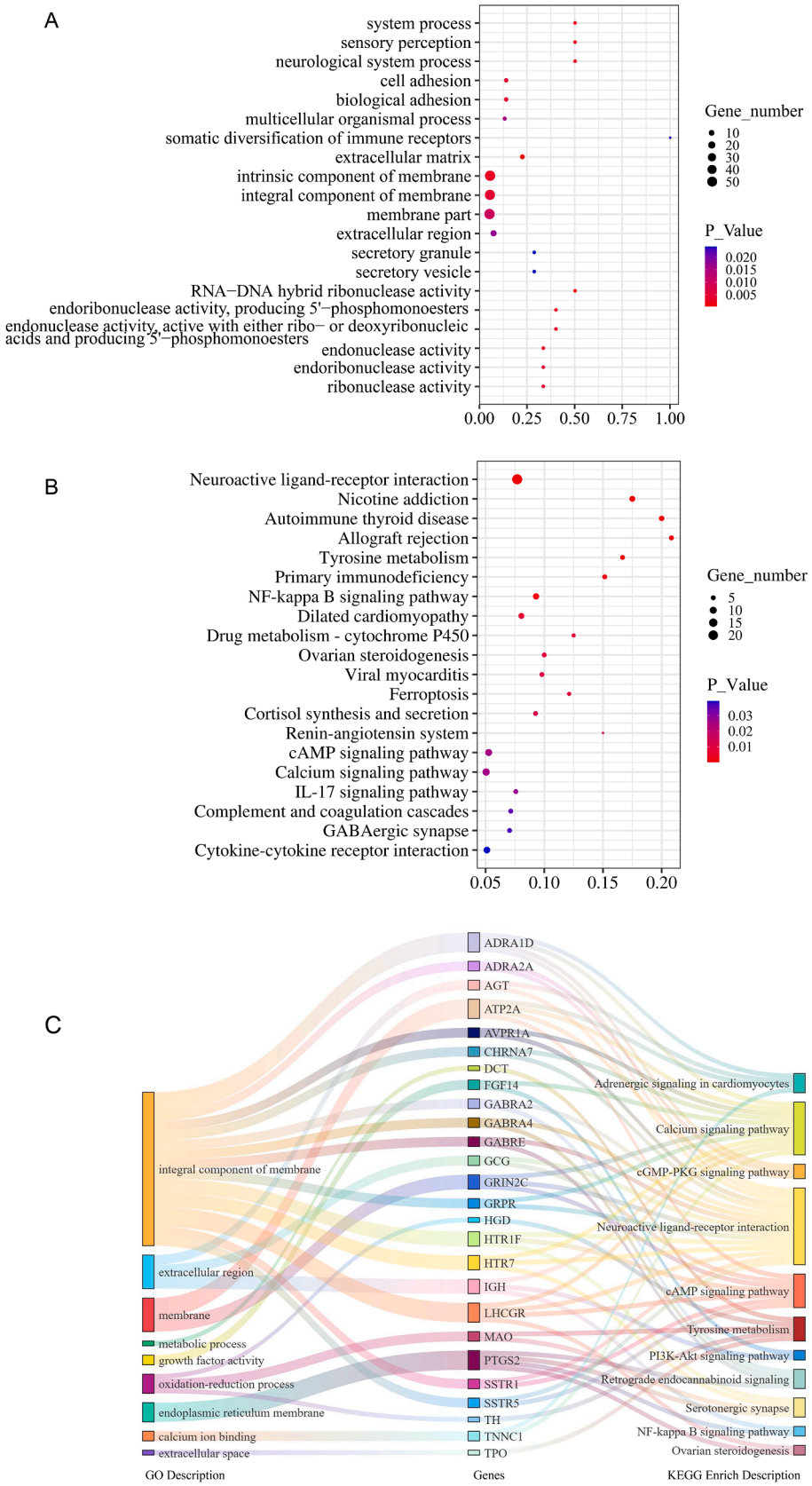

Fig. 3. Functional enrichment analysis of differentially expressed genes (DEGs). (A) Gene ontology (GO) enrichment analysis of DEGs. The top six or seven terms enriched with DEGs in each subcategory: Biological Process (BP), Molecular Function (MF), Cellular Component (CC). The horizontal coordinate represents the rich factor. (B) Kyoto Encyclopedia of Genes and Genomes (KEGG) enrichment analysis of DEGs. The top 20 signaling pathways with DEGs significantly enriched are shown, excluding those classified as human diseases in the primary classification. The horizontal coordinate represents the rich factor. (C) Description of DEGs co-enriched by KEGG pathway and GO terminology. The enrichment of important DEGs in the KEGG pathway and GO terminology is shown.

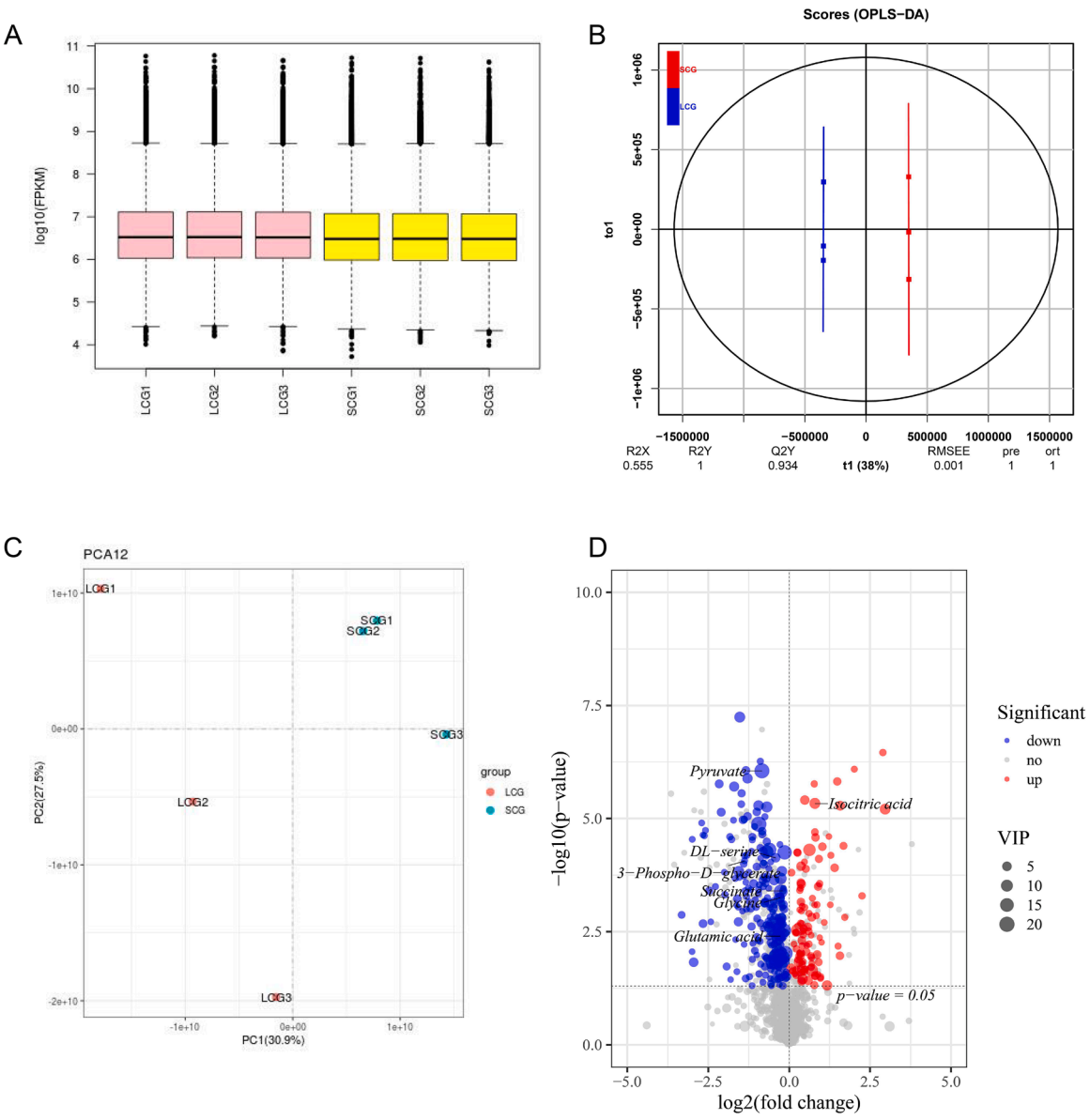

Fig. 4. Metabolome sample quality analysis. (A) Fragments per kilobase of transcript per million fragments mapped (FPKM) box plot. The difference in the overall expression of each sample can be measured by density. (B) Score scatter plot of the orthogonal partial least squares-discriminant analysis (OPLS-DA)model. R2X and R2Y represent the interpretation rate of the model for X and Y matrices; $Q^2Y \in [0,1]$. The larger the Q^2Y, the better the model prediction performance. (C) Principal component analysis (PCA). Each point in the figure represents a sample, with the horizontal coordinate indicating the value of principal component 1 and the vertical coordinate indicating the value of principal component 2. (D) Differential metabolites (DMs) volcano map analysis. The red metabolites are significantly up-regulated, whereas the blue metabolites are significantly down-regulated.

affecting LCL. Pyruvate, isocitric acid, D/L-serine, 3-phospho-d-glycerate, succinate, glycine, and glutamic acid were considered as the key metabolites. These DEGs were enriched in 233 pathways and DMs were enriched in 111 pathways. Among these, 24 pathways were coenriched with DEGs and DMs.

Luteinizing hormone (**LH**) is an important hormone that induces ovulation in females and the production of male and female steroid hormones (Qiaos et al., 2019; Shaaban et al., 2018). Genetic variants in *LHCGR* may affect oocyte maturation by altering the structure or function of the LH receptor it encodes. (Jin et al., 2023). In this study, *LHCGR* was found to play a key role in LCL. Li et al. (2013) found that *LHCGR* has an impact on egg production and reproductive performance of chickens. In females, *LHCGR* is expressed in theca cells and differentiated granulosa cells of the ovaries (Zhang et al., 2020). Single-nucleotide polymorphisms (**SNP**) in *LHCGR* may alter its gene expression or protein function, thereby affecting its biological activity and contributing to the development of polycystic ovary syndrome (**PCOS**) in women (Mutharasan et al., 2013). Alarcón-Granados et al. (2022), Makhdoomi et al. (2023), and Singh et al. (2023) also reported similar results in their studies.

Further, *AVPR1A* expression was significantly higher in the LCG than in the SCG. This gene is speculated to play a key regulatory role in the egg-laying process in geese. *AVPR1A* activates intracellular G-protein signaling pathways by binding to arginine vasopressin (**AVP**) (Caldwell et al., 2008), thereby exerting multiple physiological functions (Uhlén et al., 2015). AVP can fine-tune progesterone biosynthesis by granulosa cells (Yamamoto et al., 2023). Interestingly, in a study on mammals (including mice and humans) conducted by Jamieson et al. (2022) and Goparaju and Gragnoli (2024), *AVPR1A* was found to be associated with the occurrence of PCOS. These findings provide direction for further research on *AVPR1A*.

Yang et al. (2023b) reported that fibroblast growth factor 12 (*FGF12*)

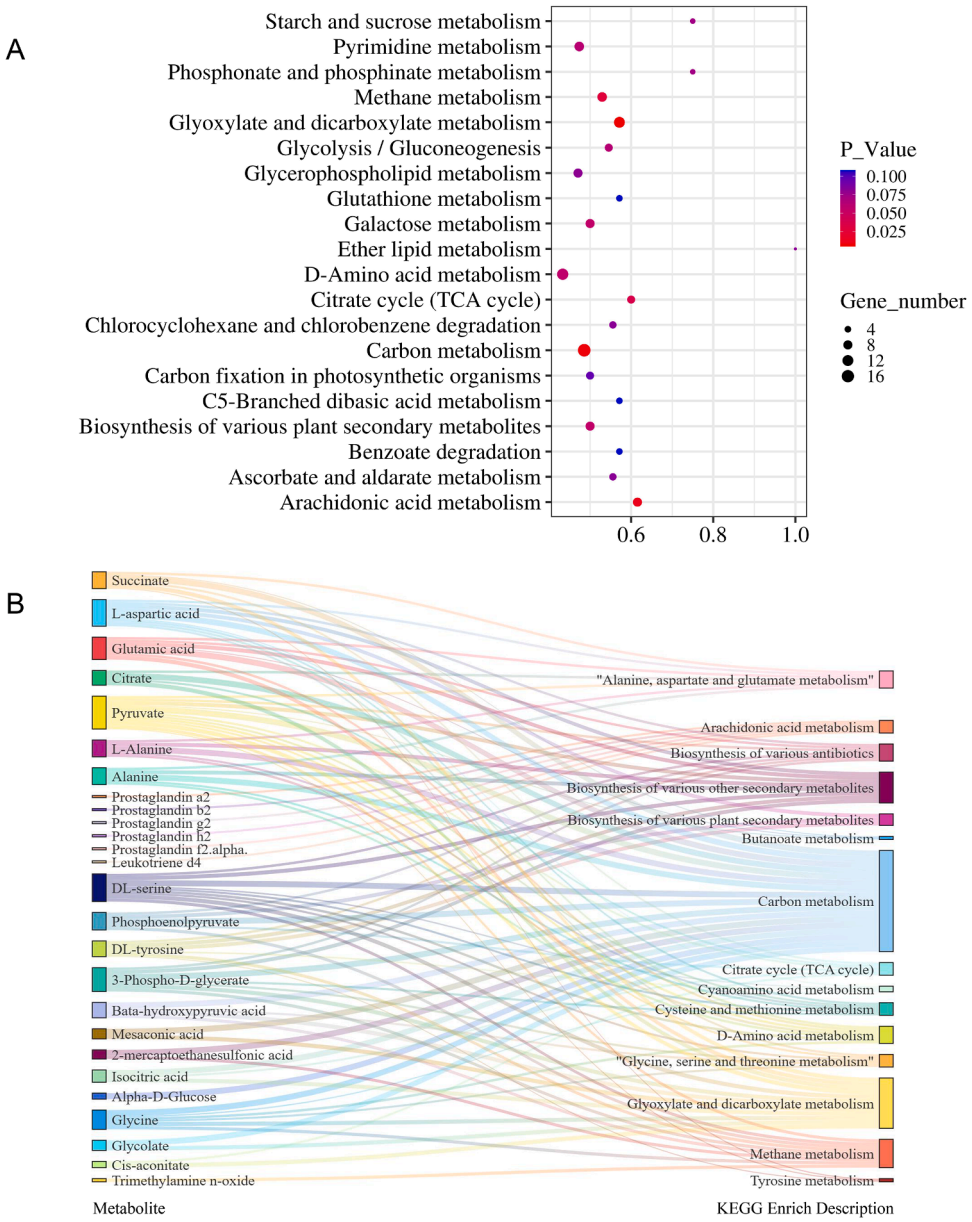

Fig. 5. Functional enrichment analysis of differential metabolites (DMs). (A) Kyoto Encyclopedia of Genes and Genomes (KEGG) enrichment analysis of DMs. Only the top 20 metabolic pathways with the most significant enrichment of DMs are shown. The horizontal coordinate represents the rich factor. (B) Description of enriched DMs by the relevant KEGG pathways. The enrichment of important DMs in the KEGG pathways is shown.

could regulate the proliferation of granulosa cells in geese. Marashi (2018) found that after sheep granulosa cells were exposed to fibroblast growth factor 8 (FGF8) and fibroblast growth factor 18 (FGF18), the expression of proteins such as activating transcription factor 1 (ATF1) and signal transducer and activator of transcription 3 (STAT3) in granulosa cells was significantly increased. In the present study, *FGF14* expression was significantly different between the two groups. As a member of the fibroblast growth factor family, we speculate that *FGF14* may exert a regulatory effect on the ovarian granulosa cells of Zi geese; however, this needs to be confirmed in further research.

Both *AVPR1A* and *LHCGR* were significantly enriched in neuroactive ligand-receptor interactions. The interaction of neuroactive ligand-receptor plays a crucial role in the egg-laying process of poultry such as chickens (Zhang et al., 2019), ducks (Tao et al., 2017) and geese (Ouyang et al., 2020). Five DEGs including *LHCGR* were significantly enriched in the ovarian steroidogenesis pathway. Bao et al. (2020) reported that ovarian steroidogenesis plays an important regulatory role in ovarian function. Further, 11 DEGs, including *LHCGR* and *FGF14* were significantly enriched in the calcium signaling pathway. Anizoba et al. (2024) suggested that calcium ions played a key role in eggshell formation. Another study in chickens (Chen et al., 2021) showed similar results. Notably, *LHCGR* and *AVPR1A* are significantly enriched in terms such as intrinsic component of membrane, integral component of membrane, and membrane part. Dai et al. (2024) had similar results in a study on follicular of pigs. Furthermore, Chen et al. (2023) found that ribonuclease activity regulates the interferon response induced by dsRNA, thereby enhancing the disease resistance function of the ovaries.

In the present study, based on the relative expression levels of DMs and the pathways related to egg-laying performance, we selected seven significant DMs that might affect the egg-laying performance of geese. Pyruvate (Alcantara da Silva et al., 2024; Zhang et al., 2024), isocitric acid, and succinate (Choi et al., 2021) are primarily involved in the TCA cycle in animals and supply energy for biological processes. 3-Phospho-d-glycerate (Wohlgemuth, 2023) and pyruvate (Alcantara da Silva

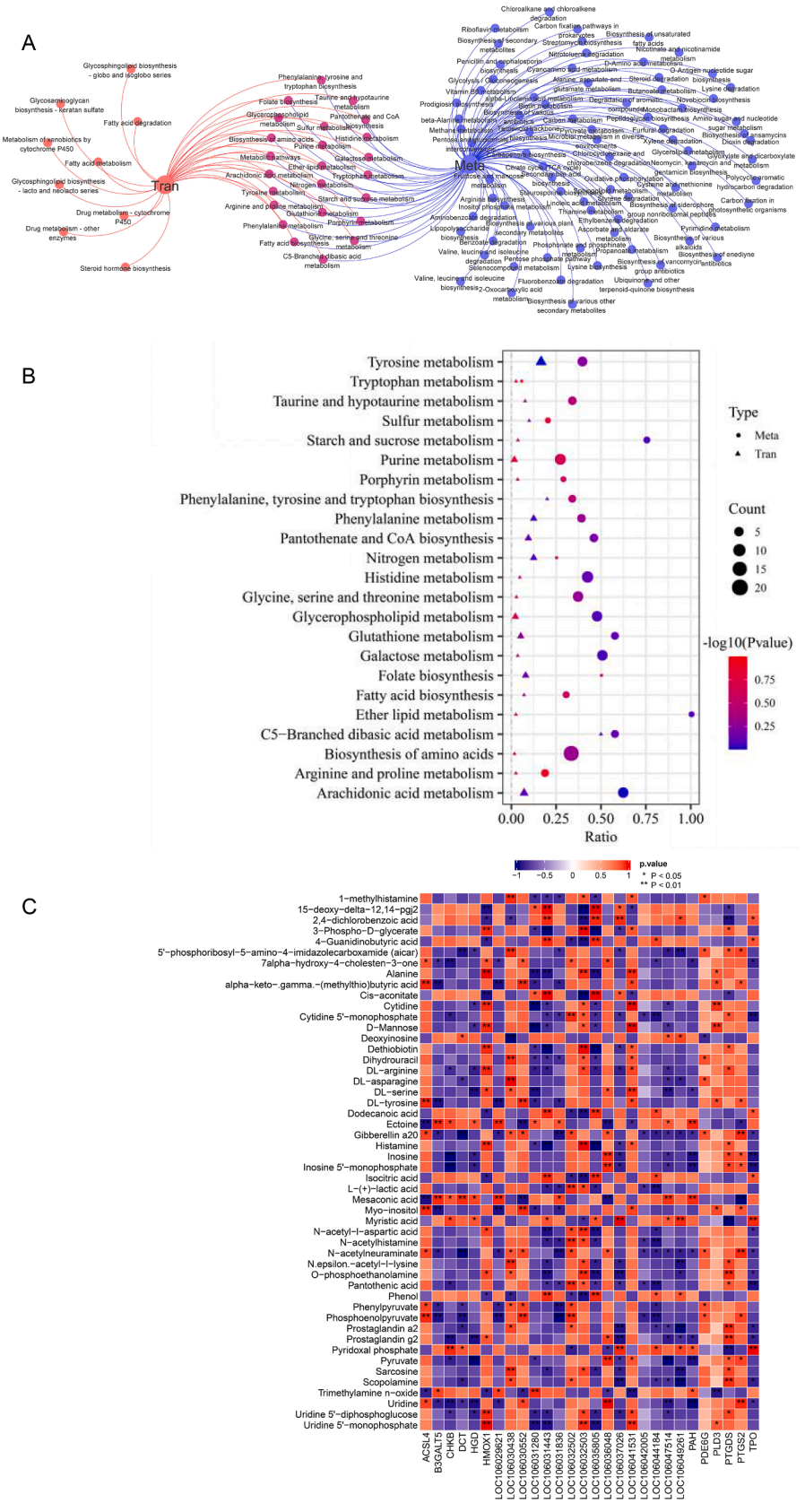

Fig. 6. Integration analysis of Kyoto Encyclopedia of Genes and Genomes (KEGG) pathways between the transcriptome and metabolome. (A) Venn diagram of KEGG enrichment pathways in the transcriptome and metabolome. Among them, the differentially expressed gene (DEG) enriched pathway only shows that classified as metabolism. (B) Pathway analysis for the coenriched DEGs and differential metabolites (DMs). The top 20 pathways of co-enrichment were shown. (C) Correlation analysis of DEGs enriched in the KEGG pathways and the top 50 DMs.

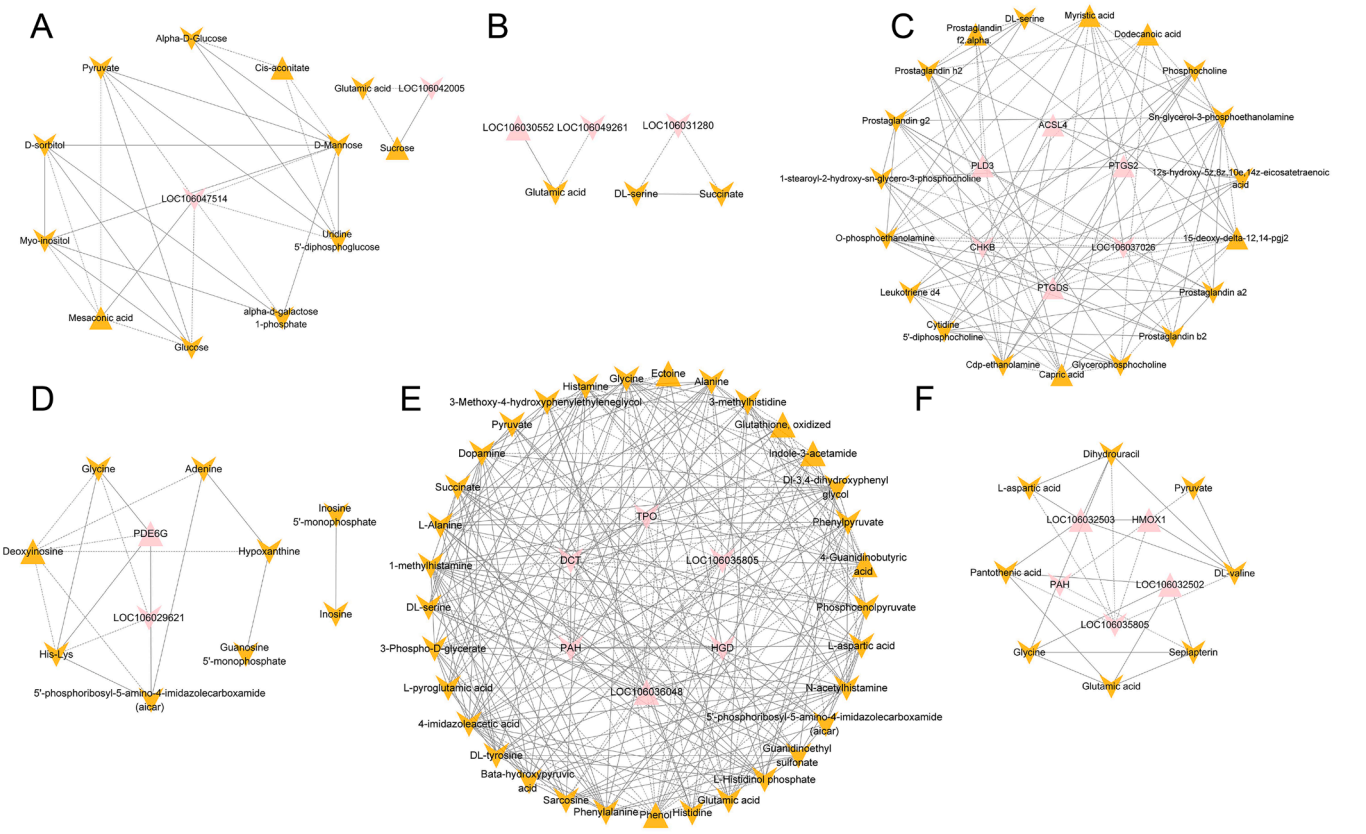

Fig. 7. Interaction network diagram of differentially expressed genes (DEG) and differential metabolites (DMs). (A) Carbohydrate metabolism, (B) Energy metabolism, (C) Lipid metabolism, (D) Nucleotide metabolism, (E) Amino acid metabolism, and (F) Coenzyme factors and vitamin metabolism according to the Kyoto Encyclopedia of Genes and Genomes (KEGG) secondary classification. The pink triangle represents mRNA up-regulation, the pink V-shape represents mRNA down-regulation, the yellow triangle represents metabolite up-regulation, the yellow V-shape represents metabolite down-regulation, dashed lines represent negative correlation, and solid lines represent positive correlation.

et al., 2024) are located at key positions in the glycolytic pathway in animals and are intermediate products of glucose catabolism. The glycolytic pathway provides energy for various biological activities and plays a crucial role during egg-laying in poultry (Liu et al., 2024). D/L-serine, glycine, and glutamic acid are jointly enriched in amino acid metabolism and are important amino acids. Amino acids are the basic units used to construct proteins, which are the main nutritional components of eggs (Dermane et al., 2024). In addition, metabolites such as pyruvate, D/L-serine, glycine, and glutamic acid are inseparably related to the secretion of protein hormones such as gonadotropin-releasing hormone, follicle-stimulating hormone, and luteinizing hormone (Sha et al., 2024). In the present study, pyruvate, D/L-serine, 3-phospho-d--glycerate, succinate, glycine, and glutamic acid showed a significant downward trend in the LCG, whereas isocitric acid showed a significant upward trend. We thus speculated that as egg production increases, a large number of amino acids and lipid metabolites are used for egg synthesis, resulting in decreased levels of these metabolites in the ovaries (Liu et al., 2022). The relationships among these factors will be the focus of future research.

To investigate the correlations between transcriptomic and metabolomic data, and elucidate the potential synergistic mechanisms through which DEGs and DMs regulate pathways underlying egg-laying performance in Zi geese, we conducted integrated transcriptomic and metabolomic association analysis. We determined that the *ACSL4*-phosphoenolpyruvate pair is the key gene-metabolite pairs affecting goose LCL. As reported by Han et al. (2024) *ACSL4* is a marker gene for ferroptosis, which is closely related to lipid peroxidation. Lipid peroxidation may lead to granulosa cell apoptosis, reduce LH synthesis and inhibit follicular maturation (Aten et al., 1992). Studies by Przygrodzka et al. (2025) have shown that blocking the dephosphorylation of phosphoenolpyruvate to pyruvate–a critical step in ATP generation–disrupts LH function. This might explain why ACSL4 and phosphoenolpyruvate are highly correlated during continuous egg-laying in geese. While the ACSL4-phosphoenolpyruvate pair is hypothesized to link granulosa cell apoptosis and LH synthesis in follicular cells, the specific gene-metabolite relationship in geese clutch trait requires further experimental validation.

Conclusion

AVPR1A, FGF14, and *LHCGR* are the key genes regulating LCL in geese. In the ovaries, pyruvate, isocitric acid, D/L-serine, 3-phospho-d-glycerate, succinate, glycine, and glutamic acid are considered molecular markers that affect the goose LCL, and the *ACSL4*–phosphoenolpyruvate pair emerged as a significant gene-metabolite interaction. Overall, these findings provide a scientific basis for future improvements in the reproductive efficiency of geese. Additionally, the results regarding the metabolomic analysis need to be further validated in studies with larger sample sizes.

Funding

This work was supported by the China Aericultural Research System (CARS-42-24), Bio-breeding Industry Innovation and Development Project of Heilongjiang Province (2024), and Heilongjiang Bayi Agricultural University Graduate Innovative Research Project (YJSCX2024-Y42).

Declaration of competing interest

Conflicts of interest are not addressed in this article.

Supplementary materials

Supplementary material associated with this article can be found, in the online version, at doi:10.1016/j.psj.2025.105210.

References

Alarcón-Granados, M.C., Moreno-Ortiz, H.., Rondón-Lagos, M., Camargo-Villalba, G.E., Forero-Castro, M., 2022. Study of *LHCGR* gene variants in a sample of Colombian women with polycystic ovarian syndrome: a pilot study. J. King Saud Univ. Sci. 34, 102202.

Alcantara da Silva, J.V., Ispada, J.., Nociti, R.P., da Fonseca Junior, A.M., de Lima, C.B., Dos Santos, E.C., Chiaratti, M.R., Milazzotto, M.P., 2024. The central role of pyruvate metabolism on the epigenetic maturation and transcriptional profile of bovine oocytes. Reproduction 167, e230181.

Anizoba, N.W., Ikeh, N..E., Ezenwosu, C., Amaefule, B.C., Obinna, A.L., Ugwu, S.O.C., 2024. Egg characteristics, blood parameters and tibia mineralization of laying hens fed varying dietary levels of limestone and periwinkle shell. Iran. J. Appl. Anim. Sci. 14.

Aten, R.F., Duarte, K..M., Behrman, H.R., 1992. Regulation of ovarian antioxidant vitamins, reduced glutathione, and lipid peroxidation by luteinizing hormone and prostaglandin F2α. Biol. Reprod. 46, 401–407.

Bao, Q., Yao, Y., Weng, K., Zheng, M., Zhang, Y., Zhang, Y., Chen, G., Xu, Q., 2022. Research note: comparison on laying behavior and clutch traits among Zhedong white geese (*Anser cygnoides*), Sichuan white geese (*Anser cygnoides*), and Hungarian geese (*Anser anser*). Poult. Sci 101, 101594.

Bao, X., Song, Y., Li, T., Zhang, S., Huang, L., Zhang, S., Cao, J., Liu, X., Zhang, J., 2020. Comparative transcriptome profiling of ovary tissue between black Muscovy duck and white Muscovy duck with high- and low-egg production. Genes 12, 57.

Bello, S.F., Xu, H.., Guo, L., Li, K., Zheng, M., Xu, Y., Zhang, S., Bekele, E.J., Bahareldin, A.A., Zhu, W., Zhang, D., Zhang, X., Ji, C., Nie, Q., 2021. Hypothalamic and ovarian transcriptome profiling reveals potential candidate genes in low and high egg production of white Muscovy ducks (*Cairina moschata*). Poult. Sci. 100, 101310.

Caldwell, H.K., Lee, H..J., Macbeth, A.H., Young 3rd, W.S., 2008. Vasopressin: behavioral roles of an "original" neuropeptide. Prog. Neurobiol. 84, 1–24.

Chen, X., Sun, X., Chimbaka, I.M., Qin, N., Xu, X., Liswaniso, S., Xu, R., Gonzalez, J.M., 2021. Transcriptome analysis of ovarian follicles reveals potential pivotal genes associated with increased and decreased rates of chicken egg production. Front. Genet. 12, 622751.

Chen, Z., Yin, M., Jia, H., Chen, Q., Zhang, H., 2023. *ISG20* stimulates anti-tumor immunity via a double-stranded RNA-induced interferon response in ovarian cancer. Front. Immunol. 14, 1176103.

Choi, I., Son, H., Baek, J.H., 2021. Tricarboxylic acid (TCA) cycle intermediates: regulators of immune responses. Life 11, 69.

Dai, J., Pang, M., Cai, J., Liu, Y., Qin, Y., 2024. Integrated transcriptomic and metabolomic investigation of the genes and metabolites involved in swine follicular cyst formation. Front. Vet. Sci. 10, 1298132.

Dermane, A., Eloh, K., Palanga, K.K., Tchakinguena Adjito, D., N'nanle, O., Karou, D.S., Kpanzou, T.A., Caboni, P., 2024. Comparative metabolomic profiling of eggs from 3 diverse chicken breeds using GC-MS analysis. Poult. Sci. 103, 103616.

Goparaju, P., Gragnoli, C., 2024. Implication of vasopressin receptor genes (*AVPR1A* and *AVPR1B*) in the susceptibility to polycystic ovary syndrome. J. Ovarian Res. 17, 214.

Han, S., Yu, C., Qiu, M., Xiong, X., Peng, H., Song, X., Hu, C., Zhang, Z., Xia, B., Yang, L., Chen, J., Zhu, S., Li, W., Yang, C., 2024. *USP13* regulates ferroptosis in chicken follicle granulosa cells by deubiquitinating *ATG7*. Poult. Sci 103, 104209.

Hao, H., Ren, X., Ma, Z., Chen, Z., Yang, K., Wang, Q., Liu, S., 2024. Comprehensive analysis of the differential expression of mRNAs, lncRNAs, and miRNAs in Zi goose testis with high and low sperm mobility. Poult. Sci. 103, 103895.

Jamieson, B.B., Moore, A..M., Lohr, D.B., Thomas, S.X., Coolen, L.M., Lehman, M.N., Campbell, R.E., Piet, R., 2022. Prenatal androgen treatment impairs the suprachiasmatic nucleus arginine-vasopressin to kisspeptin neuron circuit in female mice. Front. Endocrinol. 13, 951344.

Jin, H., Yang, H., Zheng, J., Zhou, J., Yu, R., 2023. Post-trigger luteinizing hormone concentration to positively predict oocyte yield in the antagonist protocol and its association with genetic variants of *LHCGR*. J. Ovarian Res. 16, 189.

Li, D.Y., Zhang, L.., Yang, M.Y., Xu, H.L., Yin, H.D., Li, Y., Zhu, Q., 2013. Effect of luteinizing hormone/choriogonadotropin receptor (*LHCGR*) gene on chicken reproductive traits. Mol. Biol. Rep. 40, 7111–7116.

Liu, H., Yang, Q., Guo, R., Hu, J., Tang, Q., Qi, J., Wang, J., Han, C., Zhang, R., Li, L., 2022. Metabolomics reveals changes in metabolite composition of duck eggs under the impact of long-term storage. J. Sci. Food Agric. 102, 4647–4656.

Liu, Q., Song, Y., Ma, J., Mabrouk, I., Zhou, Y., Hu, J., Sun, Y., 2024. The combination of RNA-seq transcriptomics and data-independent acquisition proteomics reveal the mechanisms and function of different gooses testicular development at different stages of laying cycle. Poult. Sci. 103, 104007.

Makhdoomi, M.J., Shah, I..A., Rashid, R., Rashid, A., Singh, S., Shah, Z.A., Ganie, M.A., 2023. Effect modification of *LHCGR* gene variant (rs2293275) on clinico-biochemical profile, and levels of luteinizing hormone in polycystic ovary syndrome patients. Biochem. Genet. 61, 1418–1432.

Marashi, F.A., 2018. Effects of Fibroblast Growth Factor 8 and 18 on Ovine Ovarian Granulosa Cell Function. Master Diss. Univ. Montreal, Montreal, QC, Canada.

Mutharasan, P., Galdones, E., Penalver Bernabé, B., Garcia, O.A., Jafari, N., Shea, L.D., Woodruff, T.K., Legro, R.S., Dunaif, A., Urbanek, M., 2013. Evidence for chromosome 2p16.3 polycystic ovary syndrome susceptibility locus in affected women of European ancestry. J. Clin. Endocrinol. Metab. 98, E185–E190.

Ouyang, Q., Hu, S., Wang, G., Hu, J., Zhang, J., Li, L., Hu, B., He, H., Liu, H., Xia, L., Wang, J., 2020. Comparative transcriptome analysis suggests key roles for 5-hydroxytryptamine receptors in control of goose egg production. Genes 11, 455.

Przygrodzka, E., Bhinderwala, F., Powers, R., McFee, R.M., Cupp, A.S., Wood, J.R., Davis, J.S., 2025. Metabolic control of luteinizing hormone-responsive ovarian steroidogenesis. J. Biol. Chem. 301, 108042.

Qiao, J., Han, B., 2019. Diseases caused by mutations in luteinizing hormone/chorionic gonadotropin receptor. Prog. Mol. Biol. Transl. Sci. 161, 69–89.

Sha, Y., Liu, X., Li, X., Wang, Z., Shao, P., Jiao, T., He, Y., 2024. Succession of rumen microbiota and metabolites across different reproductive periods in different sheep breeds and their impact on the growth and development of offspring lambs. Microbiome 12, 172.

Shaaban, Z., Jafarzadeh Shirazi, M.R., Nooranizadeh, M.H., Tamadon, A., Rahmanifar, F., Ahmadloo, S., Ramezani, A., Zamiri, M.J., Jahromi, I.R., Sarvestani, F.S., Hosseinabadi, O.K., 2018. Decreased expression of arginine-phenylalanine-amide-related peptide-3 gene in dorsomedial hypothalamic nucleus of constant light exposure model of polycystic ovarian syndrome. Int. J. Fertil. Steril. 12, 43–50.

Singh, S., Kaur, M., Beri, A., Kaur, A., 2023. Significance of *LHCGR* polymorphisms in polycystic ovary syndrome: an association study. Sci. Rep. 13, 22841.

Tao, Z., Song, W., Zhu, C., Xu, W., Liu, H., Zhang, S., Huifang, L., 2017. Comparative transcriptomic analysis of high and low egg-producing duck ovaries. Poult. Sci. 96, 4378–4388.

Uhlén, M., L. Fagerberg, B. M. Hallström, C. Lindskog, P. Oksvold, A. Mardinoglu, Å. Sivertsson, C. Kampf, E. Sjöstedt, A. Asplund, I. Olsson, K. Edlund, E. Lundberg, S. Navani, C. A. Szigyarto, J. Odeberg, D. Djureinovic, J. O. Takanen, S. Hober, T. Alm, P. H. Edqvist, H. Berling, H. Tegel, J. Mulder, J. Rockberg, P. Nilsson, J. M. Schwenk, M. Hamsten, K. von Feilitzen, M. Forsberg, L. Persson, F. Johansson, M. Zwahlen, G. von Heijne, J. Nielsen, and F. Pontén. 2015. Tissue-based map of the human proteome. Science. 347:1260419.

Wang, J., Liu, Z., Cao, D., Liu, J., Li, F., Han, H., Han, H., Lei, Q., Liu, W., Li, D., Wang, J., Zhou, Y., 2023. Elucidation of the genetic determination of clutch traits in Chinese local chickens of the Laiwu black breed. BMC Genomics 24, 686.

Wohlgemuth, R., 2023. Advances in the synthesis and analysis of biologically active phosphometabolites. Int. J. Mol. Sci. 24, 3150.

Wolc, A., Bednarczyk, M., Lisowski, M., Szwaczkowski, T., 2010. Genetic relationships among time of egg formation, clutch traits and traditional selection traits in laying hens. J. Anim. Feed Sci. 19, 452–459.

Wolc, A., Jankowski, T., Arango, J., Settar, P., Fulton, J.E., O'Sullivan, N.P., Dekkers, J.C. M., 2019. Investigating the genetic determination of clutch traits in laying hens. Poult. Sci. 98, 39–45.

Wu, X., Pan, X., Cao, S., Xu, F., Lan, L., Zhang, Y., Lian, S., Yan, M., Li, A., 2019. iTRAQ-based quantitative proteomic analysis provides insights into strong broodiness in Muscovy duck (*Cairina moschata*) combined with metabolomics analysis. J. Proteomics. 204, 103401.

Xi, Y., Wang, L., Qi, J., Wei, B., Han, X., Lu, Y., Hu, S., He, H., Han, C., Zhu, Y., Hu, J., Liu, H., Wang, J., Li, L., 2023. Comprehensive transcriptomic and metabolomic analysis of the effect of feed restriction on duck sternal development. Poult. Sci. 102, 102961.

Yamamoto, K., Nakano, Y., Iwata, N., Soejima, Y., Suyama, A., Hasegawa, T., Otsuka, F., 2023. Stimulatory effects of vasopressin on progesterone production and BMP signaling by ovarian granulosa cells. Biochem. Biophys. Res. Commun. 667, 132–137.

Yan, X., Liu, H., Hu, J., Han, X., Qi, J., Ouyang, Q., Hu, B., He, H., Li, L., Wang, J., Zeng, X., 2022. Transcriptomic analyses of the HPG axis-related tissues reveals potential candidate genes and regulatory pathways associated with egg production in ducks. BMC Genomics 23, 281.

Yang, H., Li, Y., Yuan, J., Ni, A., Ma, H., Wang, Y., Zong, Y., Zhao, J., Jin, S., Sun, Y., Chen, J., 2023a. Research note: genetic parameters for egg production and clutch-related traits in indigenous Beijing-You chickens. Poult. Sci. 102, 102904.

Yang, G., Li, S., Zhao, Q., Chu, J., Zhou, B., Fan, S., Shi, F., Wei, X., Hu, X., Zheng, X., Liu, Z., Zhou, X., Tao, Y., Li, S., Mou, C., 2021. Transcriptomic and metabolomic insights into the variety of sperm storage in oviduct of egg layers. Poult. Sci. 100, 101087.

Yang, W., Yu, S., Peng, J., Chang, P., Chen, X., 2023b. FGF12 regulates cell cycle gene expression and promotes follicular granulosa cell proliferation through ERK phosphorylation in geese. Poult. Sci. 102, 102937.

Yuan, X., Hu, S., Li, L., Liu, H., He, H., Wang, J., 2020. Metabolomic analysis of SCD during goose follicular development: implications for lipid metabolism. Genes 11, 1001.

Zhan, H., Xiong, Y., Wang, Z., Dong, W., Zhou, Q., Xie, S., Li, X., Zhao, S., Ma, Y., 2022. Integrative analysis of transcriptomic and metabolomic profiles reveal the complex molecular regulatory network of meat quality in Enshi black pigs. Meat Sci 183, 108642.

Zhang, T., Chen, L., Han, K., Zhang, X., Zhang, G., Dai, G., Wang, J., Xie, K., 2019. Transcriptome analysis of ovary in relatively greater and lesser egg producing Jinghai yellow chicken. Anim. Reprod. Sci. 208, 106114.
Zhang, X., Ge, J., Wang, Y., Chen, M., Guo, X., Zhu, S., Wang, H., Wang, Q., 2024. Integrative omics reveals the metabolic patterns during oocyte growth. Mol. Cell. Proteomics. 23, 100862.
Zhang, Z., Wu, L., Diao, F., Chen, B., Fu, J., Mao, X., Yan, Z., Li, B., Mu, J., Zhou, Z., Wang, W., Zhao, L., Dong, J., Zeng, Y., Du, J., Kuang, Y., Sun, X., He, L., Sang, Q., Wang, L., 2020. Novel mutations in LHCGR (luteinizing hormone/choriogonadotropin receptor): expanding the spectrum of mutations responsible for human empty follicle syndrome. J. Assist. Reprod. Genet. 37, 2861–2868.